Available online at www.sciencedirect.com
SCIENCE DIRECT®
Blood Cells, Molecules, and Diseases 32 (2004) 176–181
BLOOD CELLS, MOLECULES, & DISEASES
www.elsevier.com/locate/ybcmd

A single amino acid change in the binding pocket alters specificity of an anti-integrin antibody AP7.4 as revealed by its crystal structure

Sona Vasudevan,[1] Reha Celikel, Zaverio M. Ruggeri, Kottayil I. Varughese, and Thomas J. Kunicki*

Department of Molecular and Experimental Medicine, The Scripps Research Institute, La Jolla, CA 92037, USA

Submitted 16 April 2003

(Communicated by E. Beutler, M.D., 22 October 2003)

Abstract

Monoclonal antibody (mAb) AP7.4 is an anti-integrin antibody recombinantly expressed in *Escherichia coli* specific to $\alpha_v\beta_3$. It is known that in a variety of RGD-containing molecules, ligand specificity is regulated by structural determinants within the immediate vicinity of the RGD sequence. To better understand the role of the RGD sequence in integrin specificity, we report here the three-dimensional structure of Fab of mAb AP7.4 to a resolution of 2.25 Å. The crystals belong to a triclinic space group P1 and the volume of the unit cell is consistent with the presence of two Fab molecules in it. The RGD sequence is located at the tip of a flexible loop in the complementary determining region (CDR-3) of the heavy chain. It has been shown that specific recognition of RGD ligands by their receptors is influenced mainly by the conformation of the tripeptide RGD and the amino acid residues flanking it on either side. Hence, the flexibility of the RGD-carrying loop observed in the crystal structure may stem from the fact that the antibody molecule mimics the function of these cell adhesion molecules.

Keywords: Amino acid; Anti-integrin antibody; Crystal structure.

Introduction

Integrins are receptors at the cell surface that mediate cell adhesion and cell interactions [1,2]. Structurally, integrins are membrane glycoprotein heterodimers each consisting of a noncovalently associated α and β subunits [3–8]. The specificity of an integrin is dictated in large by its αβ subunit composition. It is well known that these receptors mediate a wide range of cell adhesion events that are the most crucial processes in the area of fundamental human biology and hemostasis. A thorough understanding of the integrin function requires some insight into the complementary binding sites on the adhesive proteins that are recognized by these receptors. One commonly recognized site is a tripeptide sequence RGD, first identified in fibronectin [9,10] and subsequently in numerous other adhesive molecules, that includes fibrinogen, vitronectin, type-I collagen, osteopontin and von Willebrand factor [2,8], each of which contain one or more RGD sequences. The RGD-containing peptides have been instrumental in the identification of the integrin receptors. This motif is recognized by $\alpha_{IIb}\beta_3$ and at least six other RGD-cognitive integrins $\alpha_v\beta_1$, $\alpha_v\beta_3$, $\alpha_v\beta_5$, $\alpha_v\beta_6$, $\alpha_v\beta_8$ and $\alpha_5\beta_1$ [4,11–13]. Although each of these integrins recognize the RGD motif, each also exhibits selective affinities for the variety of natural ligands that contain the RGD sequence. Recognition of the RGD-containing ligands by the individual receptors is influenced by the conformation of the RGD tripeptide in addition to the amino acids flanking the RGD sequence.

Since the discovery of the importance of the RGD motif in platelet function and thrombogenesis, there has been a great deal of interest in the characterization of natural or synthetic products that contain or mimic the RGD motif. Antibodies have been instrumental in exploring receptor–ligand interactions. Antibodies directed to the ligand-binding site of the integrin receptors may mimic receptor–ligand interactions in vivo. We have undertaken one such structural

* Corresponding author. Department of Molecular and Experimental Medicine, The Scripps Research Institute, 10550 North Torrey Pines Road, Maildrop MEM-150, La Jolla, CA 92037. Fax: +1-858-784-2174.
E-mail addresses: vasudevs@helix.nih.gov (S. Vasudevan), tomk@scripps.edu (T.J. Kunicki).
[1] Current address: National Center for Biotechnology Information, National Institutes of Health, Bethesda, MD 20892, USA.

1079-9796/$ - see front matter © 2003 Elsevier Inc. All rights reserved.
doi:10.1016/j.bcmd.2003.04.001

Table 1
Recombinant Fab molecules that belong to the AP7 series

Fab	H3 sequence	Ligand
OPG2	HPFYRYDGGN	$\alpha_{IIb}\beta_3$
AP7	HPFYRGDGGN	$\alpha_{IIb}\beta_3$, $\alpha_v\beta_3$
AP7.4	HPFYRGDGGA	$\alpha_v\beta_3$

approach to study the specificity of the various receptors to their ligands by the use of a panel of antibody fragments called the AP7 series, containing either an RGD or RYD sequence in the complementarity determining (CDR) of the antibody heavy chain. This paper reports the crystal structure of one such antibody fragment of the AP7 series (AP7.4) that contains an RGD sequence in the H3 loop. Table 1 summarizes the different recombinant Fab molecules that belong to the AP7 series with their respective ligands they recognize.

Murine monoclonal antibody (mAb) OPG2, the parent molecule of the AP7 series, is a paradigm of natural RGD ligands and binds specifically to $\alpha_{IIb}\beta_3$. The 2.0-Å crystal structure of the antigen-binding fragment (Fab) of the parent antibody OPG2 has shown that the reactive RYD (Arg 103–Tyr 104–Asp 105) tripeptide is at the tip of an extended loop of the third CDR of the heavy chain (H3) [14]. When compared to other RGD-containing ligands, the RYD of OPG2 is unique in that the side chains are fixed in a stable orientation. The H3 loop is shown to exist in two different conformations. The authors have speculated that the two distinct conformations could represent two binding modes of OPG2 in its bound and unbound forms. An interesting feature of the RYD motif is that Asp 105 makes a hydrogen bond with Asn 108 of the H3 loop thereby stabilizing the loop conformation and the ligand potentially recognizes the RYD motif in a particular orientation. Substitution of Tyr 104 to Glycine in Fab AP7 has been shown to retain the specificity of the integrin to $\alpha_{IIb}\beta_3$. Crystal structure of OPG2 Fab in complex with a peptide from the β3 subunit has also been reported [15]. Significant conformational changes have been reported to have occurred on binding to the peptide. The atomic positions of the H3 loop that includes the RYD motif have not been determined in the reported crystal structure attributed to the flexibility of the H3 loop.

AP7.4, the structure of which is discussed in this paper, is similar to AP7 with the exception of one amino acid substitution in the H3 loop (HPFYRGDGGN in AP7 versus HPFYRGDGGA in AP7.4), an nonionic Alanine residue in place of Asn 108. A single amino acid substitution seems to be sufficient to change the specificity of AP7.4 to $\alpha_v\beta_3$. The substitution of Asn 108 by Ala would eliminate the hydrogen bond formed by Asp 105 and thereby lead to another conformation of the H3 loop changing the specificity of AP7.4. The results also argue that $\alpha_v\beta_3$ is quite selective with respect to the directionality of Arg 103 and Asp 105 side chains. The most important generalizations that have resulted from analysis of the AP7 series is that the amino acid composition immediately adjacent to the RGD tripeptide in the macromolecular ligands can change the specificity of the ligand for β3 integrins.

To address this structurally, we have crystallized and determined the three-dimensional structure of Fab of AP7.4 to high resolution.

Materials and methods

Crystallization

The purified Fab was concentrated to 18 mg/ml and used for various crystallization trials. The protein stock was stored in a solution containing 10 mM ammonium acetate pH 7.3 with 0.25 mM EDTA. Sizable rectangular-shaped crystals (0.1 × 0.1 × 1 mm) suitable for X-ray diffraction analysis were grown in hanging drops on equilibration with a reservoir solution containing 15% PEG 8000, 20 mM sodium citrate pH 5.6, 12% isopropanol and 30 mM barium chloride.

Data collection and data statistics

X-ray diffraction data to a resolution of 2.25 A were measured on a MAR image plate at beam line 7–1 at the Stanford Synchrotron Radiation Laboratory. Crystals belong to a Triclinic space group P1, with unit cell parameters a = 56.479 Å; b = 57.978 Å; c = 79.224 Å; α = 109.95; β = 87.98° and γ = 107.56°. The unit cell dimensions are consistent with two Fab molecules per asymmetric unit with a solvent content of 48% and a Mathews coefficient of 2.4. The data collection statistics is presented in Table 2.

Structure determination

The structure was solved using molecular replacement techniques. The variable and the constant domains of pdb entry 1OPG (ref for pdb) were used as a starting search model to obtain the phases by molecular replacement. The correct rotation and translation functions were obtained using the program x-plor [16]. Molecular replacement calculations were performed with data in the resolution range 10–4.

The initial rotation function was refined by Patterson correlation analysis implemented in x-plor [16]. The variable

Table 2
Data collection statistics

Data collection	
Space group	P1
Cell constants	a = 56.479 Å; b = 57.978 Å; c = 79.224 Å; α = 109.953; β = 87.977; γ = 107.561
Maximum resolution (Å)	2.25
Total no. of measured reflections	201,358
Unique reflections	39,070
Completeness (%)	90.8
Rsym (%)	5.7
I/sigma2	3.2

and constant domains of the heavy and light chains were treated as independent rigid groups. The overall orientation of the Fab that was assembled for molecular replacement was subjected to a rigid body minimization in four rigid groups with data in the resolution range 8–3 Å. The packing of the Fab molecules in the asymmetric unit was inspected visually using program Setor [17]. No steric clashes were observed that could not be adjusted by minor structural adjustments. The R-factor at the end of refinement was 35%. A complete refinement was carried out at this stage and an electron density map was computed. At this stage, the correct amino acid residues differing from OPG2 were modeled into the electron density.

Model building and refinement

Six cycles of interactive model building followed by refinement was carried out using programs O [18] and x-plor [16]. For the first few cycles, the model was subjected to about 160 cycles of powell minimizations followed by simulated annealing from 3000 to 300 K with a time-step of 0.005 s. The simulated annealing was followed by 40 cycles of positional refinement. The last few steps consisted of refinement at room temperature only. Restrained B-factor refinement was carried out before computing electron density maps for interpretation.

The initial model was built into Fo–Fc omit maps from which 10% of the model was omitted from the phase calculation. This is to remove model bias. The refinement process was monitored by the use of both conventional R and R-free where 5% of the reflections were deleted to generate the test set. Non-crystallographic symmetry (NCS) restraints were imposed on the constant domains during the first few cycles of refinement resulting in a map of improved quality and phases.

Results

The crystal structure of the Fab fragment of AP7.4 has been determined to a resolution of 2.25 Å. AP7.4 assumes an overall immunoglobulin fold that is typical for all antibody fragments. Fig. 1 presents the overall trace of the two molecules and the packing of the molecules in the unit

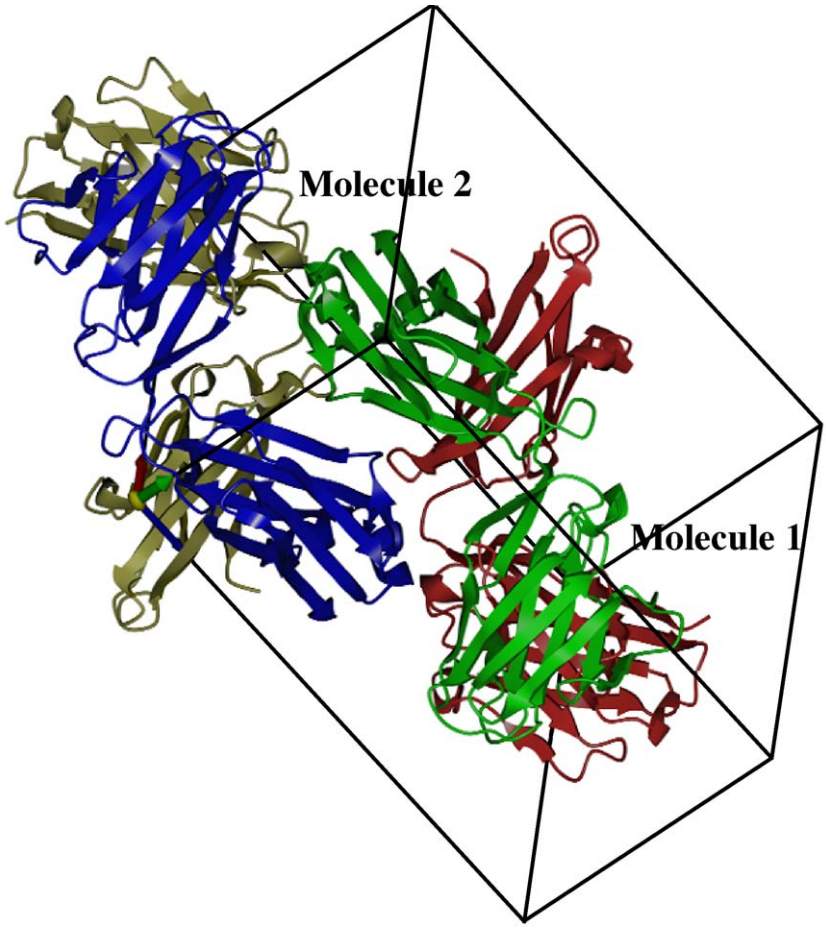

Fig. 1. Overall trace and packing of the two molecules in the crystallographic asymmetric unit of the crystal. The light chains of molecules 1 and 2 are shown in purple and green, respectively, and the heavy chains of the two molecules are shown in yellow and blue, respectively. The molecules are represented as ribbons generated using the program SETOR [17].

Table 3
Refinement statistics

Refinement	
Resolution range (Å)	8.0–2.25
R-cryst (%)	22.1
R-free (%)	28.4
No. of nonhydrogen protein atoms	6345
No. of solvent molecules	228
Rms deviations from ideality	
Bond lengths	0.008
Bond angles (°)	1.4

cell of the crystal. The final R-factor for 6345 protein atoms and 228 solvent molecules is 0.22 and an R-free of 0.28 for data in the range 8–2.25 Å. The final refinement statistics is presented in Table 3. The geometry and stereochemistry of the protein main chain dihedral angles are presented as a plot (called the Ramachandran plot) in Fig. 2 [19]. The residues (84.5%) are clustered in the energetically favored regions of the Ramachandran plot. However, one light chain residue L-51 from complementarity-determining region CDR-L2 of both molecules is found in the disallowed region (antibody numbering scheme of Kabat et al. [20] is used throughout this paper).

Based on a pair-wise comparison of two crystallographically independent molecules in the asymmetric unit, only small changes are observed in the relative disposition of the variable light and heavy chain domains. The elbow angles, that is, the angle between the pseudo-twofold axes of the variable and the constant domains as calculated by program ALIGN [21], are 166° and 165° for molecules 1 and 2, respectively. The interface angles, that is, the angle between the two variable and the two constant domains, are 160° and 155° for molecule 1 and 166° and 150° for molecule 2, respectively. The overall root mean squared deviation between the two molecules is 0.38 Å.

An analysis of the six antigen-binding loops or CDRs in several Fabs has shown that the main chain conformations are determined by a few specific residues along with the length of the loop. Five of the six antigen-binding loops (L-CDR1, L-CDR2, L-CDR3, H-CDR1 and H-CDR2) are observed only in a few main chain conformations called canonical structures [22]. As a result, L-CDR1 has been found to exist in four different canonical conformations (called types 1 through 4), CDR-L2 in one, CDR-L3 in two different conformations (types 1 and 2), CDR-H1 in two (types 1 and 2) and CDR-H2 in four different conformations (types 1 through 4).

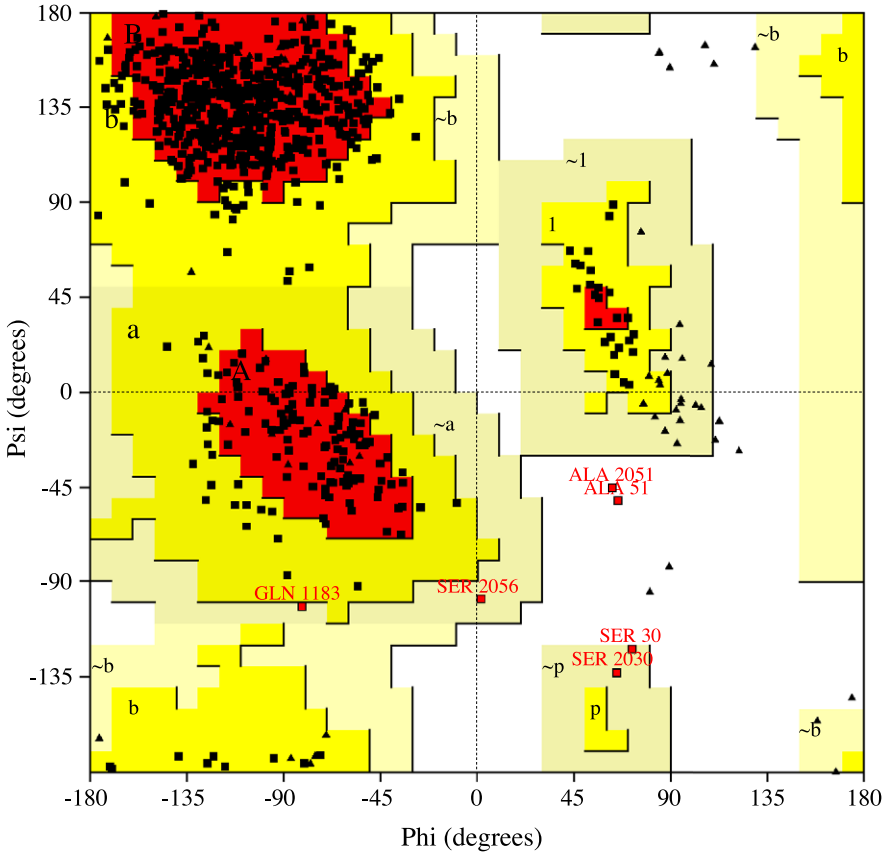

Fig. 2. Ramachandran plot of molecules 1 and 2 in the asymmetric unit of the crystal of AP7.4. The plot shows that 84.5% of the residues in the two molecules lie in the most favored regions, 14.7% lie in additionally allowed regions, 0.6% lie in generously allowed regions (residues Ser 30 (chains A and C), Ser 56 (chain A), Gln 183 (chain D)) and 0.3% lie in the disallowed regions. The two residues in the disallowed regions as discussed in the text are 51 of chains A and C that belong to CDR-L2 of the two molecules. The plot was generated using the program PROCHECK [19].

Another interesting analysis on the loop conformations was carried out by Vargas-Madrazo and Paz-Garcia [23]. Their analysis carried out on 381-Ig sequences shows that the structural repertoire of immunoglobulins is restricted to the preferential use of a few canonical structure classes. The possible functional significance of their analysis was studied by analyzing the correspondence between the observed canonical structural repertoire and the type of antigen recognized. Based on the above-mentioned classification schemes, an analysis of the six antigen-binding loops in AP7.4 was carried out. The CDRs in AP7.4 Fab showed that the loops can be classified to belong to standard canonical conformations as follows: CDRs—L1, L2, L3, H1 and H2 belong to classes 2, 1, 1, 1 and 3, respectively. Although no canonical conformation is defined for the CDR3 of the heavy chain as this is the most variable among the CDR loops in terms of its sequence and length, Shirai et al. [24] have suggested classifications based on the length of the loop. AP7.4 is unique because the length of its H3 loop is about 17 amino acids, which is at the higher end compared to most antibodies. The loop has RGD at its tip and is extremely flexible based on its temperature factors and lacks strong electron density for this region.

Discussion

Several interesting points have emerged from comparing the structures of AP7.4 and the parent molecule of the AP7 series, OPG2 (PDB entry 1OPG). As discussed earlier, the only difference in the primary sequence between the two molecules lies in CDR3 of the heavy chain, residues H99–H108 (HPFYR*G*DGG*A* in AP7.4 and HPFR*Y*DGG*N* in OPG2, the residues that differ are bolded). Major rearrangement of the CDRs seem to have occurred in AP7.4 as indicated by the root mean squared deviations between the two structures, AP7.4 and OPG2. The results are presented in Table 4. The overall rmsd between Fabs AP7.4 and OPG2 is 1.53 Å although that for Fv is 0.66 and 0.86 Å for the constant domains of the Fabs. Fig. 3 presents the superimposition of AP7.4 and OPG2.

The differences between the two structures are also indicated by the significant differences in their elbow angles (the two-fold rotation axes relating the variable and the constant domains), which is 166 in AP7.4 and only about 152 in OPG2. This 14° difference in the elbow bend is significant as already reflected in the high rms deviations between them. Table 4 summarizes the elbow bends and the domain dispositions. The maximum displacement in the Fv

Table 4
Domain dispositions and elbow angles

Fab	VL–VH	CL–CH	Elbow bend
OPG2	164	179	152
AP7.4 (Mol 1)	160	155	166
AP7.4 (Mol 2)	166	150	165

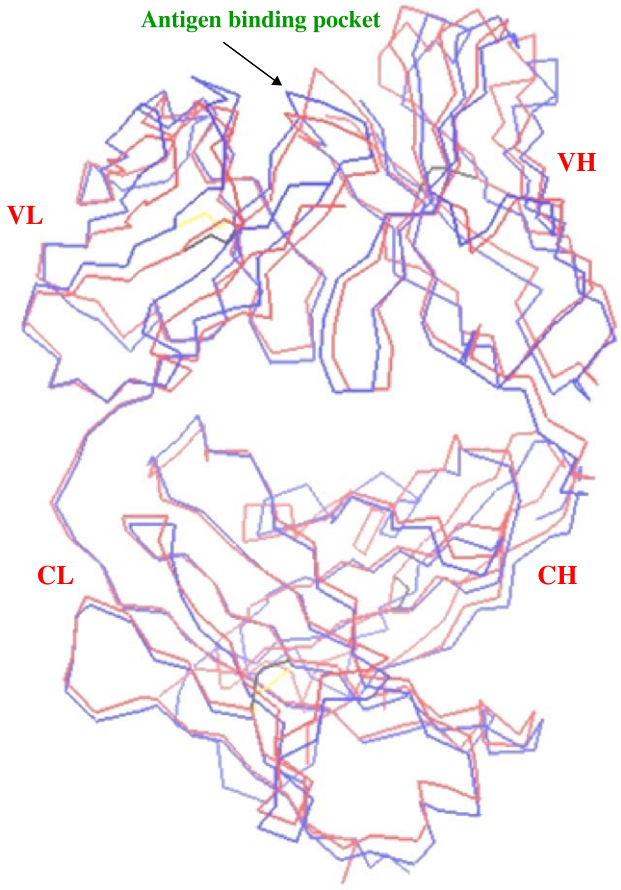

Fig. 3. Superposition of the structures of AP7.4 and the parent molecule OPG2. The overall rmsd between the two structures is about 1.53 Å. The trace of AP7.4 is shown in blue while that of OPG2 is shown in orange. Variable light, variable heavy, constant light and constant heavy are denoted as VL, VH, CL and CH, respectively. The figure was generated using the program SETOR [17].

portion of the Fabs lies in the CDR loops L1 and L2 of the light chain and H2 and H3 of the heavy chains. Maximum displacements of 1.2 Å and up to 2 Å are observed for residues in CDR-L1 and L2, respectively (residues 27–29 in L1 and 56–58 in L2), when the C-α was superimposed. Displacements up to 1.5 Å are observed for residues in CDR-H2 of the heavy chain (residues 55–57). The CDR-H3 loop is quite different between the two structures. Although residues 102–107 of AP7.4 are flexible, indicated by the weak electron density, the positions of the RGD can be ascertained. In OPG2, the H3 loop is shown to protrude about 12 Å from the base of the binding site and seems to be predominantly involved in binding to the receptor. On examination of all the solved structures of Fabs deposited in the protein data bank [25], the length of the H3 loop varies anywhere between 4 and 31 in humans and 2–19 in mice with average sizes ranging approximately between 12 and 10 residues [26,27]. However, it is interesting to see that the H3 loops of Fabs with similar lengths and sequence still adopt different conformations based on the antigen they recognize. The loops vary from an open

conformation to an extended conformation like seen in OPG2. In contrast, the H3 loop in AP7.4 seems to be more involuted and forms a binding surface to accommodate the antigen. The RGD that is at the tip of the loop is flexible and adopts different conformations in its bound form. The striking differences in the binding interface cause the change in the specificity in the Fab of AP7.4 which no longer recognizes $\alpha_{IIb}\beta 3$.

An analogy can be drawn between RGD-containing molecules that recognize integrins (like the AP7 series) and disintegrins, which are a family of platelet aggregation inhibitors found in snake venoms [28]. McLane et al. [29] have studied the importance of the RGD-containing loop in Echistatin and Eristostatin for recognition of $\alpha_{IIb}\beta_3$ and $\alpha v\beta 3$. Their study has shown that the width and the shape of the RGD-containing loop are important determinants of ligand specificity. The width of the RGD loop is determined to be the distance between the cα residues flanking either sides of the RGD motif. Hence, it is evident that residues in the immediate vicinity of the RGD motif play a crucial role in regulating ligand specificity.

In the case of AP7.4, the shape of the H3 loop is altered due to the presence of an alanine residue at position 108 instead of Asn, thus eliminating a crucial H-bond observed between aspartic acid at position 105 and the Asn in OPG2. The similarities in binding between AP7.4 and other natural ligands that contain RGD sequences, and the fact that we now have two of the three-dimensional structures of two members of the AP7 series determined to high resolution, make the AP7 derivatives an excellent paradigm for future studies aimed at further exploring the molecular basis of RGD ligand specificity.

Acknowledgments

This study was supported by NHLBI grant HL46979 (TJK) and grants HL55375, GM54246 (KIV). S. Vasudevan was supported by International Human Frontier Science Program long term fellowship.

References

[1] R.O. Hynes, Integrins: versatility, modulation, and signaling in cell adhesion, Cell 69 (1992) 11–25.
[2] R.O. Hynes, Integrins: a family of cell surface receptors, Cell 48 (1987) 549–554.
[3] M.E. Hemler, VLA proteins in the integrin family: structures, functions, and their role on leukocytes, Annu. Rev. Immunol. 8 (1990) 365–400.
[4] E. Ruoslahti, Integrins, J. Clin. Invest. 87 (1991) 1–5.
[5] T.A. Springer, Adhesion receptors of the immune system, Nature 346 (1990) 425–434.
[6] S.M. Albelda, C.A. Buck, Integrins and other cell adhesion molecules, FASEB J. 4 (1990) 2868–2880.
[7] M.A. Arnaout, Structure and function of the leukocyte adhesion molecules CD11/CD18, Blood 75 (1990) 1037–1050.
[8] E. Ruoslahti, M.D. Pierschbacher, New perspectives in cell adhesion: RGD and integrins, Science 238 (1987) 491–497.
[9] M.D. Pierschbacher, E. Ruoslahti, Cell attachment activity of fibronectin can be duplicated by small synthetic fragments of the molecule, Nature 309 (1984) 30–33.
[10] M.D. Pierschbacher, E. Ruoslahti, Influence of stereochemistry of the sequence Arg-Gly-Asp-Xaa on binding specificity in cell adhesion, J. Biol. Chem. 262 (1987) 17294–17298.
[11] S. Cheng, W.S. Craig, D. Mullen, et al., Design and synthesis of novel cyclic RGD-containing peptides as highly potent and selective integrin $\alpha_{IIb}\beta_3$ antagonists, J. Med. Chem. 37 (1994) 1–8.
[12] M. Busk, R. Pytela, D. Sheppard, Characterization of the integrin alpha v beta 6 as a fibronectin-binding protein, J. Biol. Chem. 267 (1992) 5790–5796.
[13] S.L. Nishimura, R. Pytela, Characterization of the integrin $\alpha_V\beta_8$, Mol. Biol. Cell 4 (1993) 285 (Suppl.).
[14] R. Kodandapani, B. Veerapandian, T.J. Kunicki, K.R. Ely, Crystal structure of the OPG2 Fab: an anti-receptor antibody that mimics an RGD cell adhesion site, J. Biol. Chem. 270 (1995) 2268–2273.
[15] R. Kodandapani, L. Veerapandian, C.-Z. Ni, C.-K. Chiou, R.M. Whittal, T.J. Kunicki, K.R. Ely, Conformational change in an anti-integrin antibody: structure of OPG2 Fab bound to a β3 peptide, Biochem. Biophys. Res. Commun. 251 (1998) 61–66.
[16] A.T. Brunger, P.D. Adams, G.M. Clore, W.L. DeLano, P. Gros, R.W. Grosse-Kunstleve, J.S. Jiang, J. Kuszewski, M. Nilges, N.S. Read, R.J. Read, L.M. Rice, T. Simonson, G.L. Warren, Crystallography and NMR system: a new software suite for macromolecular structure determination, Acta Crystallogr., Sect. D 54 (1998) 905–921.
[17] S.V. Evans, SETOR: hardware-lighted three-dimensional solid model representations of macromolecules, J. Mol. Graphics 11 (1993) 134–138.
[18] T.A. Jones, J.Y. Zou, S.W. Cowan, M. Kjeldgaard, Improved methods for building protein models in electron density maps and the location of errors in these models, Acta Crystallogr., Sect. A 46 (1991) 585–593.
[19] R.A. Laskowski, M.W. MacArthur, D.S. Moss, J.M. Thornton, PROCHECK: a program to check the stereochemical quality of protein structures, J. Appl. Crystallogr. 26 (1993) 283–291.
[20] E.A. Kabat, T.T. Wu, H. Bilofsky, Sequences of Immunoglobulin Chains, NIH publication National Institutes of Health, 1979, pp. 80–2008.
[21] Y. Satow, G.H. Cohen, E.A. Padlan, D.R. Davies, Phosphocholine binding immunoglobulin Fab McPC603. An X-ray diffraction study at 2.7 A, J. Mol. Biol. 190 (1986) 593–604.
[22] C. Chothia, A.M. Lesk, Canonical structures for the hypervariable regions of immunoglobulins, J. Mol. Biol. 196 (1987) 901–917.
[23] E. Vargas-Madrazo, E. Paz-Garcia, Modifications to canonical structure sequence patterns: analysis for L1 and L3, Proteins 47 (2002) 250–254.
[24] H. Shirai, A. Kidera, H. Nakamura, Structural classification of CDR-H3 in antibodies, FEBS Lett. 399 (1996) 1–8.
[25] H.M. Berman, J. Westbrook, Z. Feng, G. Gilliland, T.N. Bhat, H. Weissig, I.N. Shindyalov, P.E. Bourne, The protein data bank, Nucleic Acids Res. 28 (2000) 235–242.
[26] T.T. Wu, G. Johnson, E.A. Kabat, Length distribution of CDRH3 in antibodies, Proteins 16 (1993) 1–7.
[27] G. Johnson, T.T. Wu, Preferred CDRH3 lengths for antibodies with defined specificities, Int. Immunol. 10 (1998) 1801–1805.
[28] C.P. Blobel, J.M. White, Structure, function and evolutionary relationship of proteins containing a disintegrin domain, Curr. Opin. Cell Biol. 4 (1992) 760–765.
[29] M.A. McLane, S. Vijaykumar, C. Marcinkiewicz, J.J. Calvete, S. Niewiarowski, Importance of the structure of the RGD-containing loop in the disintegrins echistatin and eristostatin for recognition of $\alpha_{IIb}\beta_3$ and $\alpha_v\beta_3$ integrins, FEBS Lett. 391 (1996) 138–143.